EPiC Series in Computing

Volume 114, 2026, Pages 135–151

Proceedings of the Workshop on Mathematical Modeling and Scientific Computing

Computational Framework for Simulating Quorum-Regulated Growth of Mixed Bacterial Cultures

Ivan Shevkun[1], Anna Maslovskaya[1], and Christina Kuttler[2]

[1] Innopolis University, Innopolis, Russia
iv.shevkun@innopolis.ru, a.maslovskaya@innopolis.ru
[2] Technische Universität München, München, Germany
kuttler@ma.tum.de

Abstract

Quorum sensing, that is the exchange of signal molecules whose concentration reflects the population density, allows bacteria to switch on collective programs in a coordinated way, including virulence. Suppression of this communication by enzymes that degrade the signal is considered as an alternative to antibiotics, and the source of the enzyme can be another bacterial population. In this paper, we propose a reaction-diffusion model of joint growth of two bacterial species on a nutrient medium. The first species produces signal molecules and, with a delay, its own enzyme that degrades them. The second species does not take part in quorum sensing, but constantly secretes the enzyme and quenches the foreign signal. The species compete for a shared substrate. The problem is solved by an implicit splitting scheme in spatial variables; computations are performed by a multithreaded C++ program, and visualization and processing of the results are done in MATLAB. Computational experiments showed that without quorum sensing the outcome of competition is decided at the growth front of the colony. Within the parameter range studied here, quorum quenching by the second species increases with enzyme production and reduces the duration of the coordinated state, but does not eliminate it. Control simulations, in which the second species competes for the substrate but does not produce the enzyme, allowed us to separate the quenching effect from competition and to identify three regimes depending on the fraction of the signal-producing species in the initial population: no effect, partial and complete quorum suppression.

1 Introduction

Quorum sensing is a mechanism that bacteria use to coordinate their behavior. It is based on the production, release and detection of signal molecules. In Gram-negative bacteria, the role of such molecules is often played by N-acyl homoserine lactones (AHL). While the population density is low, diffusion keeps the signal concentration low, so the bacterial cells remain in their ground state. When the density grows, the AHL concentration exceeds a threshold value, a positive feedback is triggered, and the colony switches on, in a coordinated way, programs that make no sense for a single cell: production of virulence factors, biofilm formation, bioluminescence [21, 24]. For a number of pathogens, it is reaching the quorum that turns the population into a virulent state, and this makes the mechanism an attractive target for therapy.

V. Turova, A. Kovtanyuk, A. Maslovskaya and J. Zimmer (eds.), MMSC 2026 (EPiC Series in Computing, vol. 114), pp. 135–151

Suppression of communication, or quorum quenching, is considered as an alternative to antibiotics: the bacterium remains viable but loses the ability to switch on a quorum-dependent lifestyle, e.g. pathogenicity/virulence, and the selection pressure for resistance is much weaker [2, 25]. The best studied natural mechanism of this kind is related to lactonases of the AiiA family, which hydrolyze the lactone ring of AHL. The enzyme was first isolated from bacteria of the genus *Bacillus* [8] and later found in many related species, including *B. thuringiensis*, *B. cereus* and *B. mycoides* [6]. It was shown that expression of the corresponding gene makes plants resistant to quorum-dependent infection [7], and co-cultivation of a lactonase producer with a pathogen stops the accumulation of signal molecules without suppressing the growth of the pathogen itself [9]; a similar effect of *B. cereus* was described against *Pseudomonas syringae* [1]. It is important that the quenching species does not take part in signal exchange: Gram-positive bacteria use oligopeptide communication and do not sense AHL [10], so their enzyme production does not depend on the concentration of the foreign signal.

Mathematical description of quorum sensing is the subject of a wide range of works (see the review [23]). The reaction-diffusion approach allows us to take into account the spatial heterogeneity of the population. Early deterministic models considered signal production, diffusion, and degradation in spatially extended bacterial populations [5, 29]. Subsequent studies incorporated receptor binding, intracellular feedback, and the interplay between diffusion and growth [12, 14, 16, 18, 22]. Recently, the role of convection and the extracellular matrix in quorum sensing communication within biofilms was experimentally investigated, revealing that these physical factors, together with quorum quenching, modulate signal transport and heterogeneity [28]. The spatial distribution of biomass in this case is described by models of nutrient-dependent growth with degenerate diffusion [13, 15]. By combining these approaches, we previously studied quorum sensing in colonies growing on a nutrient medium [19] and colony growth under external inhibition [20], and also developed a parallel implementation of the corresponding numerical schemes [27]. However, all these works consider a single bacterial species, and quorum quenching is introduced either as the population's own enzymatic activity or as an external impact with a given distribution. To our knowledge, a model in which the source of the quenching enzyme is an independent bacterial population, growing and competing for the substrate on equal terms with the signal-producing population, has not been built before.

In this paper, we extend the reaction-diffusion model of quorum sensing to the case of two bacterial species cultivated together on a nutrient medium. The signal producer synthesizes AHL with threshold positive feedback and, in accordance with experimental data for the strain *Pseudomonas putida* IsoF [3, 11], its own enzyme that degrades the signal with a delay after activation. The quencher secretes the enzyme constantly and does not take part in communication. The species interact through two channels: competition for the shared substrate and signal degradation. We are interested in the conditions under which the quencher is able to suppress the quorum of the producer, and in how to separate this effect from ordinary competition for nutrients.

2 Biological background and conceptual problem statement

Consider the following scenario. Two bacterial cultures are inoculated into a Petri dish containing a nutrient medium. The first culture (the pathogen) produces AHL signaling molecules. These molecules are subject to natural degradation and can also be broken down by the enzyme

lactonase. The second culture (the quencher) does not participate in signal transduction but constantly secretes lactonase, which is capable of suppressing quorum sensing in the first colony. Both cultures grow on the same medium and compete for the same nutrient substrate, which links their spatial distribution and growth.

We now restate the biological background in the form in which it enters the model. Quorum sensing is a mechanism by which bacteria coordinate their behavior by exchanging signaling molecules. When the signal concentration reaches a threshold value, emergent properties of the biosystem—such as the production of virulence factors or the formation of biofilms—are triggered. For many pathogens, it is precisely the attainment of a quorum that renders the population virulent. An alternative to destroying the pathogen is to disrupt its communication – quorum quenching. Lactonase enzymes degrade AHL, with the result that the pathogen remains viable but loses its ability to act in a coordinated manner.

The selective pressure on resistance is weaker in this case than when using antibiotics [4,17]. In our system, the source of lactonase is the second culture, which does not detect AHL and therefore produces the enzyme continuously. The first culture also synthesizes its own lactonase with a delay following quorum activation, which acts as a form of self-regulation.

Figure 1 schematically illustrates the described process. The pathogen secretes AHL, which undergoes natural degradation and is also degraded by lactonase. The quencher does not sense AHL but constitutively produces lactonase, which suppresses quorum sensing in the pathogen colony. The two species also compete for the shared nutrient substrate, and the pathogen regulates its own lactonase production with a delay after quorum activation.

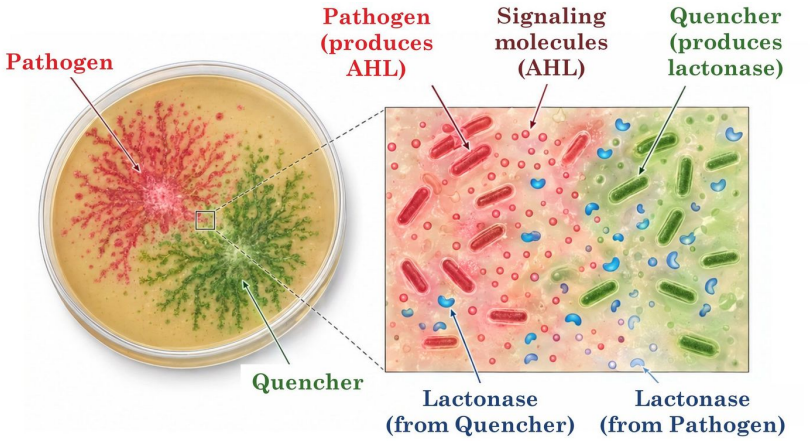


Figure 1: General schematic of the two-species system.

The key challenge in analyzing this system is that the presence of a quencher affects the pathogen in two ways simultaneously. Both species consume substrate N, so competition for the shared substrate limits the growth of the pathogen and thereby indirectly its AHL production; each biomass depends on the other even without signalling (competition for nutrients). The pathogen (species 1) produces AHL; the quencher (species 2) produces lactonase, which degrades AHL, directly reducing the signal concentration (signal interaction). Therefore, comparing "quencher present" and "quencher absent" mixes both effects and does not allow us to determine whether the reduction in quorum is caused by nutrient depletion or by enzymatic degradation of the signal. To separate these effects, we use a control scenario in which the quencher is present

and competes for the substrate but does not produce lactonase ($\beta_L = 0$). The difference between $\beta_L = 0$ and $\beta_L > 0$ isolates the net effect of quorum quenching (Fig. 2).

The objective is to construct a spatiotemporal model of the co-growth of two bacterial cultures that accounts for both competition for substrate, as well as enzymatic signal degradation, and to propose a computational framework for predicting the dynamics of such a system and identifying conditions under which a quencher is capable of suppressing quorum-dependent virulence.

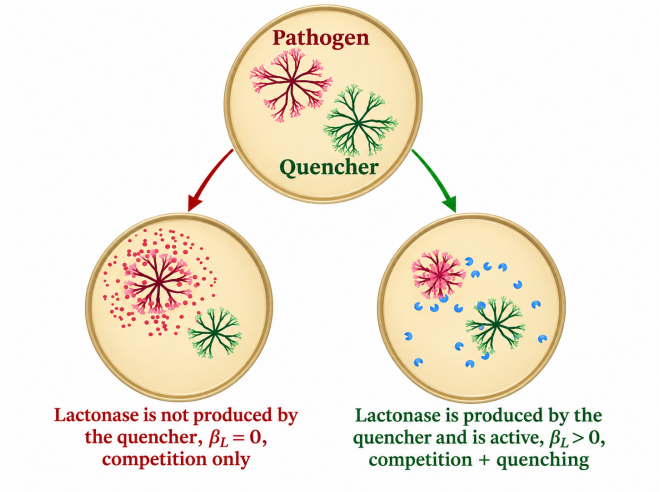


Figure 2: Separating competition from quenching.

3 Mathematical problem formulation

The problem is formulated in the square domain $\Omega = (-L, L)^2 \subset \mathbb{R}^2$ with boundary Γ on the time interval $(0, T]$. The unknown functions are: $N(x,t)$ is the concentration of the nutrient substrate, $B_1(x,t)$ and $B_2(x,t)$ are the biomass concentrations of the signal producer and the quencher, $U(x,t)$ is the concentration of signal molecules (AHL), and $L(x,t)$ is the total concentration of lactonase secreted by both species. The evolution of the biosystem is described by the following system of equations:

$$\begin{cases} \dfrac{\partial N}{\partial t} = D_N \Delta N - \nu_{N1}\, N\, B_1 - \nu_{N2}\, N\, B_2, \\ \dfrac{\partial B_i}{\partial t} = \nabla \cdot \left(\sigma_i\, N\, B_i\, \nabla B_i\right) + \nu_{Bi}\, N\, B_i, \qquad i = 1, 2, \\ \dfrac{\partial U}{\partial t} = D_U \Delta U - \gamma_U U - \gamma_{L\to U}\, L\, U + \alpha_{B1}\, B_1\, f_1(U), \\ \dfrac{\partial L}{\partial t} = D_L \Delta L - \gamma_L L + \alpha_{B1}\, B_1\, f_2(U) + \beta_L\, \alpha_{B2}\, B_2, \end{cases} \quad x \in \Omega, \quad 0 < t \le T. \tag{1}$$

The first three equations describe nutrient-dependent growth of two competing populations and generalize the Kawasaki model [15] to the case of two species. The biomass diffusion coefficient $\sigma_i N B_i$ vanishes where there is no substrate or no bacteria, so the colony expands

only at the front, where some nutrient is still left. Following [15, 27], we set $\sigma_i = \sigma_{0i}(1+\delta)$, where δ is a random variable with triangular distribution on $[-\rho, \rho]$; it is these fluctuations that lead to the branched, flower-like shape of the colonies. In the growth equations, the species are coupled only through the shared substrate: cross-diffusion and mutual displacement are not taken into account, so both species can be present at the same point. The biomass diffusion coefficient of each species depends on its own density B_i rather than on the total biomass. This form is a direct generalization of the Kawasaki model [15]. It is based on the observation that bacterial cells do not move where the nutrient concentration or the cell density is low and become active when they increase. The product σNB is the simplest form of this dependence. Since we have no data on how cells of one species affect the motility of the other, we keep this form for each species separately. With unequal initial fractions, this makes the less abundant species less mobile. In Experiments 1 and 2 and in Series A of Experiment 3 the initial fractions are equal ($\varphi = 0.5$), and this effect does not arise. In Series B, where $\varphi \neq 0.5$, the difference in motility is the same in the main and in the control ($\beta_L = 0$) simulations with the same φ. Therefore it does not affect the difference between these simulations, which shows the net effect of quorum quenching. A model with the coefficient $\sigma_i N(B_1 + B_2)$, i.e., with cross-diffusion, is a possible generalization that we leave for future work.

The last two equations describe the dynamics of the substances that determine quorum sensing [16, 19]. The coupling between the two groups of equations is one-way: the biomasses enter the sources of U and L, while the reverse influence of these concentrations on growth is not considered. The generation functions in (1) have the form

$$f_1(U) = \alpha_U + \beta_U \frac{U^k}{U_{th}^k + U^k}, \qquad f_2(U) = \beta_{L1} \frac{U^k}{(U_{th}+\varepsilon)^k + U^k}. \tag{2}$$

According to (1) and (2), the source of signal molecules is related only to species 1. The enzyme source contains two terms of fundamentally different nature. Lactonase production by species 1 is of threshold type and is induced by the signal itself, and the threshold in f_2 is shifted by ε with respect to U_{th}: in this way we take into account the delay of enzyme synthesis after the AHL burst observed in *P. putida* IsoF [11]. Production by species 2 is constant, since the Gram-positive quencher does not sense AHL and cannot switch on in response to its appearance. The normalizations $\alpha_{Bi} = 1/B_{i,\max}$ make the biomasses dimensionless.

The initial conditions are given as

$$N(x,0) = N_0, \qquad U(x,0) = U_0, \qquad L(x,0) = L_0, \tag{3}$$

$$B_1(x,0) = \varphi\, B_m \exp\left(-\frac{|x-x_1|^2}{C_1^2}\right), \qquad B_2(x,0) = (1-\varphi)\, B_m \exp\left(-\frac{|x-x_2|^2}{C_2^2}\right), \tag{4}$$

where N_0, U_0, L_0, B_m, C_1, C_2 are the parameters of the initial distributions, x_1, $x_2 \in \Omega$ are the inoculation centers, and $\varphi \in [0,1]$ is the fraction of species 1 in the inoculum. When $x_1 = x_2$, the species grow intermixed from one point. The zero-flux condition is set on Γ:

$$\left.\frac{\partial N}{\partial \mathbf{n}}\right|_\Gamma = 0, \quad \left.\frac{\partial B_i}{\partial \mathbf{n}}\right|_\Gamma = 0, \quad \left.\frac{\partial U}{\partial \mathbf{n}}\right|_\Gamma = 0, \quad \left.\frac{\partial L}{\partial \mathbf{n}}\right|_\Gamma = 0, \qquad 0 < t \le T, \tag{5}$$

where $\mathbf{n}$ is the outward normal to Γ.

To estimate the level of communication quantitatively, we introduce the fraction of the area of the species 1 colony occupied by cells with active quorum sensing:

$$Q(t) = \frac{\left|\{x \in \Omega :\ B_1 > B_c,\ U > U_{th}\}\right|}{\left|\{x \in \Omega :\ B_1 > B_c\}\right|}, \qquad B_c = 0.05 \max_\Omega B_1. \tag{6}$$

Since $Q(t)$ changes over time, together with (6) we use three integral characteristics: the cumulative quorum exposure over the observation time $E_Q = \int_0^T Q\,dt$, the final coverage $Q(T)$, and the duration of strong quorum, i.e., the state in which more than half of the colony area exhibits active quorum sensing,

$$t_{0.5} = \big|\{t \in (0,T) :\ Q(t) > 0.5\}\big|. \tag{7}$$

4 Computational framework

To solve problem (1) – (5) numerically, we use a finite-difference splitting scheme in spatial variables [30], which we previously applied to the single-species model [19, 27]. The domain is covered by a uniform grid with steps h_x, h_y, and each time step τ is divided into two half-steps: at the first one, only the derivatives in x are approximated, at the second one, only the derivatives in y. Thus the two-dimensional problem is reduced to a sequence of one-dimensional ones. At each half-step, the scheme is implicit with respect to the unknown function. The coefficients of the difference operator for B_i, which depend on N and B_i, are computed from the values at the previous half-step, the sources are treated explicitly, and the term $\gamma_{L\to U} LU$ describing signal degradation is taken implicitly in U. The resulting tridiagonal systems are solved by the sweep (Thomas) method. We checked the practical convergence of the scheme for the single-species version of the model by the Runge rule, with the spatial and time steps refined at the same time: the relative l_2 error of the solution decreases as the number of steps grows. A detailed analysis of accuracy and stability is beyond the scope of this paper. The order of computations at one time step is given below.

Iterative algorithm Computation of one time step

1: Generate the values of δ at all grid nodes.
2: For each grid row, solve by the sweep method along x the equation for N, then the equations for B_1 and B_2 with the updated N, then the equation for L, and the equation for U with the updated L. The rows are processed in parallel.
3: Generate new values of δ.
4: For each grid column, solve by the sweep method along y the equations in the same order. The columns are processed in parallel.
5: At selected steps, write the fields N, B_1, B_2, U, L to a file.

The same realization of the random field δ is used for both species, so with equal growth parameters the species differ only in their initial fraction and in the signaling system.

The scheme is well suited for parallelization: at the first half-step, the systems for different grid rows are independent, and at the second one, the systems for different columns. Therefore the rows (columns) are distributed between threads, and synchronization is needed only between the half-steps. The colony occupies the central part of the domain, and the computational load over the rows is non-uniform, so the rows are assigned to threads in turn rather than in solid blocks: such alternating partitioning balances the load better [27].

The overall structure of the computational framework is summarised in Fig. 3. The solver first reads the grid parameters, the initial distributions (3)–(4), and the model coefficients from Table 1. At every time step the two-dimensional problem is split into two one-dimensional half-steps. During the x-half-step, the random field δ is generated once and the equations are solved along each grid row in the order $N \to B_1 \to B_2 \to L \to U$, so that the updated nutrient

and biomass fields are used in the enzyme and signal equations. The y-half-step repeats the same sequence along the grid columns with a freshly generated δ. The rows and columns are distributed between threads, and synchronisation is required only at the end of each half-step. At selected time steps the fields N, B_1, B_2, U, and L are written to disk. After the time loop terminates, the saved fields are transferred to MATLAB, where the spatial distributions and the two-species overlays are visualised, and the quorum metrics $Q(t)$, E_Q, $Q(T)$, and $t_{0.5}$ are computed according to (6) and (7).

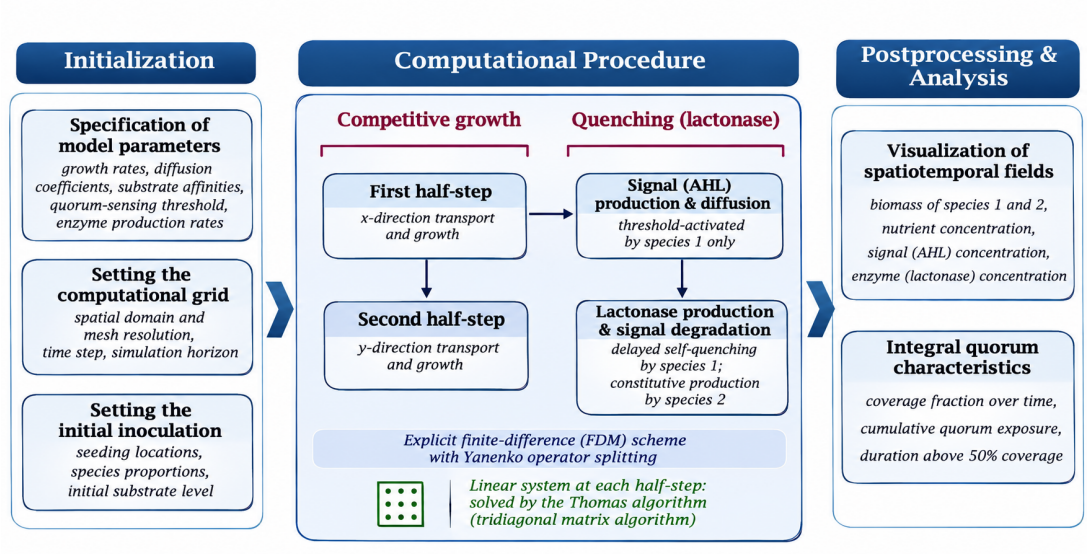


Figure 3: Functional diagram of the computational framework.

The first version of the software implementation was developed in MATLAB. In the current implementation, the computational core is moved to C++ without third-party parallelization libraries: threads are created with `std::thread`, and random variables with triangular distribution are generated with the Boost library. On an Intel Xeon w7-3455 processor (24 cores, 256 GB RAM), with 24 threads a program speedup of more than 10× was achieved for the basic Kawasaki model [27]; in the two-species model, the structure of the algorithm is the same, only the number of sweeps on each grid line changes. The fields saved by the C++ program are processed in MATLAB: distribution maps and overlays of the two species are plotted, and $Q(t)$ by formula (6) and the characteristics E_Q, $Q(T)$ and $t_{0.5}$ (7) are calculated.

5 Numerical experiments

Simulations of bacterial growth were performed in normalized view of the Kawasaki model [13, 15], where the growth parameters are equal to one. The transition to physical units is done with the factors $\kappa_t = 1$ h and $\kappa_{xy} = 10^{-10}$ m^2, so that $D_N = \sigma_0 = \kappa_{xy}/\kappa_t$ and $\nu_N = \nu_B = 1/\kappa_t$. Parameters N_0, σ_{0i}, ρ are specified to provide "flower-like" structures of bacterial colonies typical for *P. putida* [19,26]. The quorum sensing parameters correspond to the strain *P. putida* IsoF [3,11]. The parameters for *P. putida* were derived from experimental measurements, while the quencher species was introduced as a modelling construct to study the effects of quorum

quenching. Therefore its enzyme production rate is not tied to a specific strain and is varied. The parameter values are given in Table 1.

Table 1: Model and numerical scheme parameters

Parameter	Description	Exp. 1	Exp. 2	Exp. 3	Unit
Computational domain and grid					
L	domain half-size		$5 \cdot 10^{-4}$		m
T	observation time	270	270	90	h
$n_x \times n_y$	number of grid nodes		500×500		—
n_t	number of time steps	1800	1800	600	—
$h_x = h_y$	grid spacing		2		μm
τ	time step		0.15		h
Population growth					
D_N	substrate diffusion		1.0		$10^{-10}\,\mathrm{m}^2/\mathrm{h}$
σ_{01}	biomass diffusion coefficient, species 1	1.1	1.0	1.0	$10^{-10}\,\mathrm{m}^2/\mathrm{h}$
σ_{02}	biomass diffusion coefficient, species 2	0.9	1.0	1.0	$10^{-10}\,\mathrm{m}^2/\mathrm{h}$
ν_{N1}	substrate consumption, species 1		1		1/h
ν_{N2}	substrate consumption, species 2	1	0.85	1	1/h
ν_{B1}	biomass growth, species 1		1		1/h
ν_{B2}	biomass growth, species 2	1	0.85	1	1/h
ρ	fluctuation amplitude		1.0		—
Initial conditions					
N_0	initial substrate	0.35	0.35	0.7	a.u.
B_m	inoculum density		0.71		a.u.
$C_1 = C_2$	inoculum half-width		25		μm
$x_1 = x_2$	inoculation centers		$(0, 0)$		m
φ	fraction of species 1	0.5	0.5	0.5 (A) 0.1–1.0 (B)	—
U_0, L_0	initial concentrations	—	—	0	mol/L
Quorum sensing (Exp. 3)					
D_U	AHL diffusion	—	—	100	$\mu\mathrm{m}^2/\mathrm{h}$
D_L	enzyme diffusion	—	—	1	$\mu\mathrm{m}^2/\mathrm{h}$
γ_U	abiotic degradation of AHL	—	—	0.05	1/h
γ_L	abiotic degradation of enzyme	—	—	0.005	1/h
$\gamma_{L\to U}$	AHL degradation by enzyme	—	—	$1.5 \cdot 10^6$	L/(mol·h)
α_U	basal AHL production	—	—	$1.058 \cdot 10^{-7}$	mol/(L·h)
β_U	induced AHL production	—	—	$1.058 \cdot 10^{-6}$	mol/(L·h)
β_{L1}	enzyme production by species 1	—	—	$5.05 \cdot 10^{-7}$	mol/(L·h)
β_L	enzyme production by species 2	—	—	0–10^{-6} (A) $5.05 \cdot 10^{-7}$, 0 (B)	mol/(L·h)
U_{th}	quorum threshold	—	—	70	nmol/L
ε	threshold delay for enzyme	—	—	5	nmol/L
k	Hill coefficient	—	—	2.5	—
$\alpha_{B1} = \alpha_{B2}$	biomass normalization	—	—	0.667	$(\text{a.u.})^{-1}$
B_c	colony support cutoff	—	—	$0.05 \max B_1$	a.u.

Note: values centered across several columns are common to these experiments.

5.1 Competition without quorum sensing

In the first two experiments, the equations for U and L are left out, and the species interact only through the substrate: quorum sensing is not taken into account in these scenarios. Both species are inoculated at one point in equal proportions ((4) with $x_1 = x_2$, $\varphi = 0.5$) on a poor medium with $N_0 = 0.35$; the observation time is $T = 270$ h.

In Experiment 1, two bacterial species with diffusion coefficients $\sigma_{01} = 1.1$ and $\sigma_{02} = 0.9$ (in units of 10^{-10} m^2/h) grow from a single center, so the species differ only in motility. Figure 4 shows the distributions at the final time. At first, the species grow together, but species 1 moves to the periphery faster and consumes the substrate ahead of the front. Since both diffusion and biomass growth are proportional to N, species 2, which stays behind the front in the depleted zone, loses both motility and the ability to grow. So at a certain moment, the species with the lower diffusion coefficient becomes nutrient-limited, stops growing, and the other species consumes the nutrient completely. By time T, species 2 occupies only a disk with a radius of about 100 μm around the inoculation point, while the colony of species 1 reaches a radius of 350–400 μm and has a clear flower-like shape. The central part of the colony remains mixed (Fig. 4c), and the substrate inside it is fully exhausted (Fig. 4d). Thus, with nutrient-dependent diffusion, a difference of about 20 % in the coefficients turns into almost complete displacement of the slower species from the growth front. The outcome of the competition is decided early: species 2 stops growing at about $t = 120$ h, when the colony radius is about 150 μm, i.e., far from the domain boundary. The domain size was reduced to speed up the computations; on a larger domain, the picture does not change qualitatively.

In Experiment 2, two bacterial species with equal motility and different nutrient consumption rates, $\nu_{N1} = 1.0$ and $\nu_{N2} = 0.85$, grow from a single center. At a certain moment, the species with the lower consumption rate begins to lag in growth and eventually stops growing due to nutrient limitation, since the other species fully consumes the surrounding nutrient. Qualitatively, the picture repeats Experiment 1, so the distributions are not shown here.

5.2 Quorum quenching by the second species

In Experiment 3, signal interaction is added to competition. Two species grow together from one droplet, intermixed, with the same diffusion coefficient $\sigma_{01} = \sigma_{02} = 1.0$, on a richer medium with $N_0 = 0.7$ (this medium was chosen to reduce the computation time: the series require many runs, and on a richer medium the colony grows faster; at $N_0 = 0.35$ the picture remains qualitatively the same); the observation time is $T = 90$ h. Both compete for the shared substrate. Species 1 produces AHL, and when the AHL concentration exceeds the threshold $U_{th} = 70$ nmol/L, the collective program switches on. After that, species 1 starts to produce its own lactonase, that is, it also quenches its own signal (self-quenching). For this reason, quorum is not a steady state for it, but a transient on-state followed by a decline. Species 2 does not sense or produce AHL, but constantly secretes lactonase, which degrades foreign AHL. The main question of the experiment is: can quenching by species 2 interfere with quorum sensing in species 1?

Two series of simulations were performed. In Series A, the two species are taken in equal proportions ($\varphi = 0.5$), and the enzyme strength of the quencher takes the values $\beta_L = 0$, 10^{-8}, $3 \cdot 10^{-8}$, 10^{-7}, $2 \cdot 10^{-7}$, $3 \cdot 10^{-7}$, $5 \cdot 10^{-7}$, 10^{-6} mol/(L·h). The question for this series is: how potent must the quenching agent be? In Series B, the enzyme strength is fixed and equal to the enzyme production rate of the producer, $\beta_L = \beta_{L1} = 5.05 \cdot 10^{-7}$ mol/(L·h), and the proportion φ of species 1 in the initial droplet is varied, from a pure culture of the signal producer ($\varphi = 1.0$) to nine times more quencher ($\varphi = 0.1$). The step in φ was 0.1 and was refined to 0.05 and then to 0.01–0.03 near the boundaries between the regimes. The question for this series is: How large a fraction of the quencher is needed? The initial conditions (3) for the signal and the enzyme are zero. For each value of φ, a control simulation was performed: the same setup but with the enzyme switched off ($\beta_L = 0$). The role of the control is the following: at a low fraction of species 1, quorum might fail to occur simply because there are too few producers,

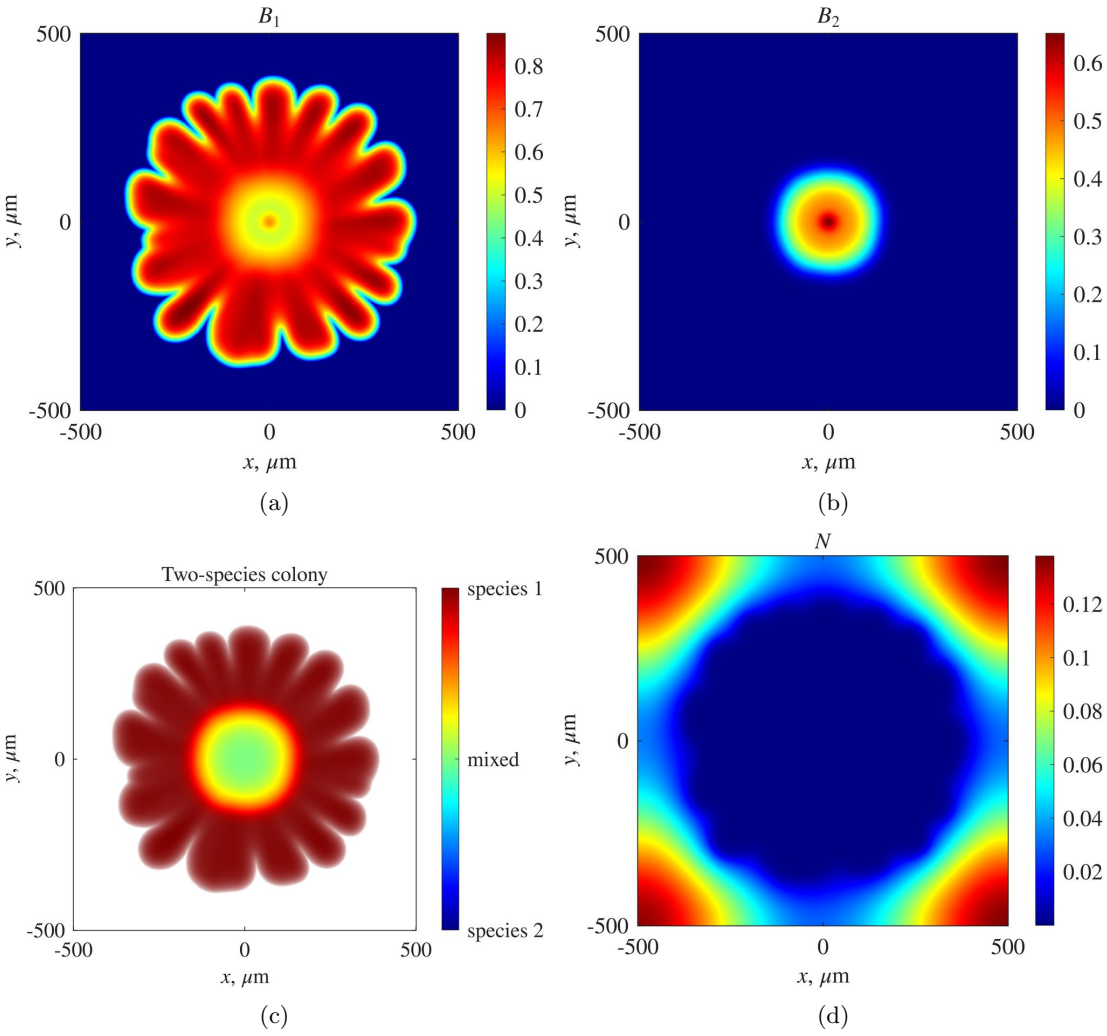


Figure 4: Distributions in Experiment 1 (species with different motility) at $t = T = 270$ h: (a) biomass of species 1 B_1; (b) biomass of species 2 B_2; (c) overlay of the two colonies, the color shows the biomass composition at a node, from pure species 2 through mixed composition to pure species 1; (d) substrate concentration N. Biomass and substrate are given in arbitrary units, the coordinates x, y are in μm.

independently of the quencher.

Figure 5 shows the distributions for $\varphi = 0.5$, $\beta_L = 5.05 \cdot 10^{-7}$ mol/(L·h) at $t = T$. Since the growth parameters of the species coincide and the same realization of the random field is used, the distributions of B_1 and B_2 are identical, and only B_1 is shown. The asymmetry between the species in this experiment comes entirely from the signaling system. Signal molecules are concentrated in a narrow ring along the colony front, where the AHL concentration is about three times higher than the threshold, while inside the colony it is low (Fig. 5b). Lactonase, on the contrary, accumulates in the center (Fig. 5c): it diffuses weakly ($D_L = 1$ μm^2/h vs $D_U = 100$ μm^2/h) and decays slowly, so it stays where the biomass has been present for the

longest time. As a result, quorum is kept only at the growing edge, where fresh biomass is ahead of the enzyme accumulation. A similar contour of high AHL concentration at the colony boundary was also observed in the single-species model [19].

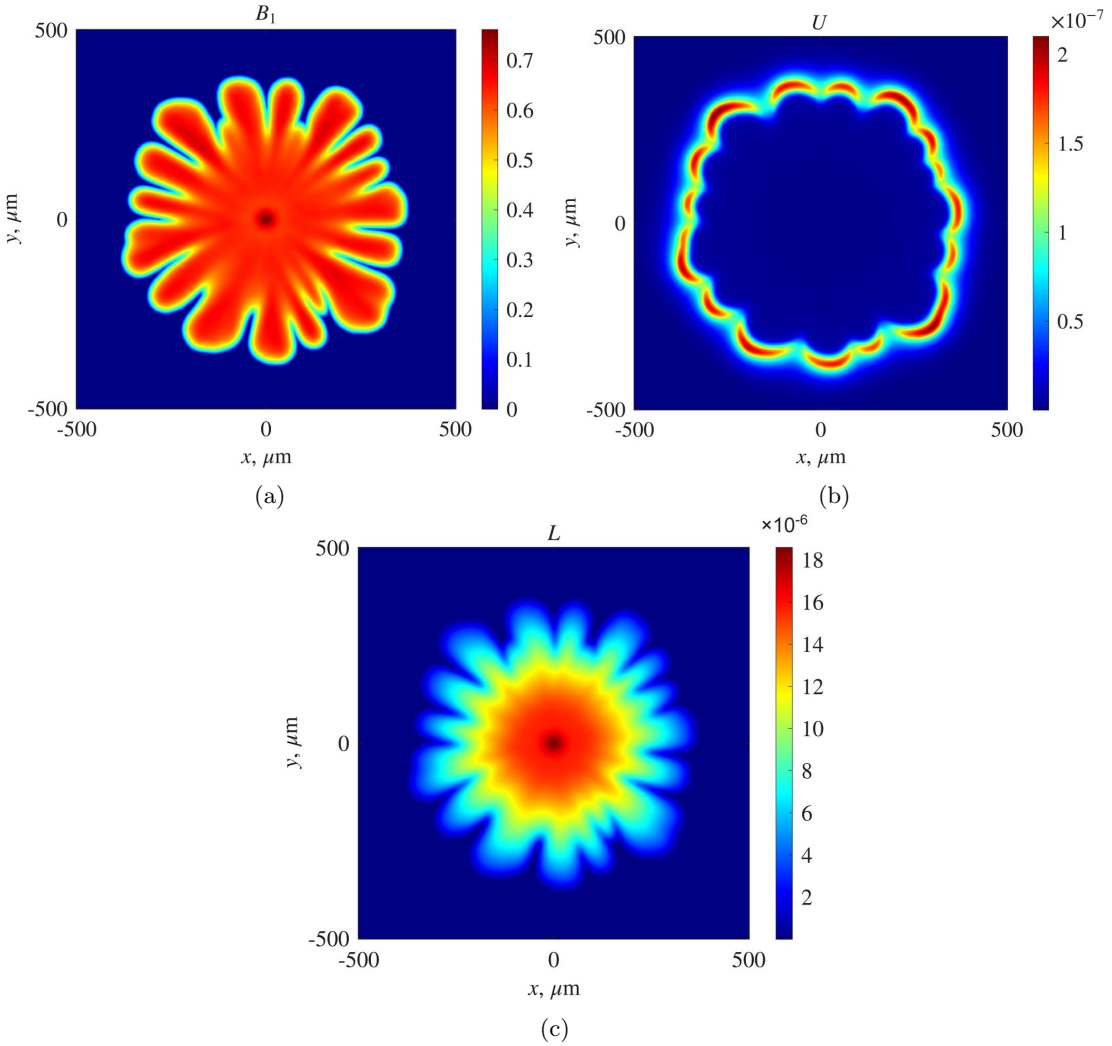


Figure 5: Distributions in Experiment 3 for $\varphi = 0.5$, $\beta_L = 5.05 \cdot 10^{-7}$ mol/(L·h) at $t = T = 90$ h: (a) biomass of species 1 B_1 in arbitrary units (the distribution of B_2 coincides with it); (b) AHL concentration U, mol/L; (c) lactonase concentration L, mol/L. The coordinates x, y are in μm.

The results of Series A are shown in Fig. 6. The quorum suppression increases smoothly, without a threshold effect: all three characteristics decrease monotonically as β_L grows over two orders of magnitude. The duration $t_{0.5}$ decreases from 36 h in the control to 11 h at $\beta_L = 10^{-6}$, and the cumulative exposure E_Q is reduced approximately by half. At the same time, even at the maximum enzyme production the colony reaches quorum: the quencher reduces the duration of the coordinated state, but does not prevent its onset. In other words, enzyme strength weakens quorum but cannot switch it off. A natural scale for β_L is given by the enzyme production of

species 1 itself. At $\beta_L = 10^{-8}$, the duration of the on-state is practically the same as in the control, and at $\beta_L \approx \beta_{L1}$, when the constant enzyme production by the quencher is comparable to the maximum induced production of the producer, it is reduced roughly by half (17 h vs 36 h).

The integral characteristics are averaged over the colony area and therefore say little about *when* each of the two quenching mechanisms comes into play. To see this, we follow the AHL concentration at two points: at the inoculation center and at a distance of 250 μm from it, which the colony front passes at about 50 h (Fig. 8 and Fig. 9). At the center the signal crosses the threshold within the first hours, and the moment of crossing almost does not depend on β_L: the foreign enzyme does not prevent the colony from reaching quorum. The difference appears in how long the signal stays above the threshold, about 16 h in the control against about 5 h at $\beta_L = 10^{-6}$ mol/(L·h). In the control, the decline has a characteristic knee: after a gentle segment the concentration falls by an order of magnitude within three or four hours. This is the moment when the own lactonase of species 1 switches on, since its production is induced by the signal itself and therefore starts with a delay after activation. As β_L grows, the knee smooths out and shifts to the left, because the constitutive enzyme of species 2 acts from the very beginning and intercepts the signal before the threshold source has time to switch on. The behavior after the decline is also indicative. In the control the concentration slowly rises again: once the signal drops below U_{th}, the threshold source of the enzyme switches off, the accumulated lactonase decays, and the signal partially recovers. With an active quencher there is no such recovery, since constitutive production does not switch off under any conditions. At the colony front the picture repeats with a time shift: the time spent above the threshold decreases from about 28 h in the control to about 11 h at $\beta_L = 10^{-6}$ mol/(L·h).

The results of Series B (Fig. 7) show why the control simulation is needed. For ($\varphi \geq 0.51$), the curves with and without species 2 coincide: the lactonase produced by species 2 has no effect, and the duration ($t_{0.5} \approx 45$) h is determined solely by the dynamics of species 1, including its own enzyme production. In the range $0.3 < \varphi \leq 0.5$, the curves diverge: at $\varphi = 0.5$, the quencher reduces $t_{0.5}$ from 36 to 17 h, and at $\varphi = 0.4$, from 18 to 5 h. The upper boundary is sharp: when φ changes from 0.50 to 0.51, $t_{0.5}$ with the quencher grows from 17 to 49 h. The control curve also goes down here, which reflects the contribution of competition and of the smaller number of signaling cells, but the gap between the curves is created by the enzyme. Finally, for $\varphi \leq 0.3$, coverage of more than half of the colony is not reached at all with the quencher, while in the control $t_{0.5}$ is 14–18 h.

Therefore, the absence of the on-state at a small fraction of the producer is caused by signal degradation and not by a lack of signaling cells. The extreme point ($\varphi = 0.1$) is especially illustrative: in the control, the producer reaches quorum by itself with the cumulative exposure ($E_Q = 12.4$) h, while with the quencher the exposure is zero.

The comparison of the two series shows that controlling the enzyme activity alone is not sufficient to suppress quorum sensing. With equal fractions of the species, even ($\beta_L = 10^{-6}$) leaves about 11 h of the on-state, while at a producer fraction of (0.3) and below, the on-state is not reached already at ($\beta_L = \beta_{L1}$). So a strategy for suppressing quorum sensing should combine both factors: the enzyme strength and the fraction of the quencher in the population. A systematic study of how these critical fractions depend on the growth and signaling parameters is beyond the scope of this paper, and we leave it for future work. Here we only note that both mechanisms – competition for the substrate and enzymatic signal degradation are present in the model, so the qualitative conclusion should not be tied to a single parameter set.

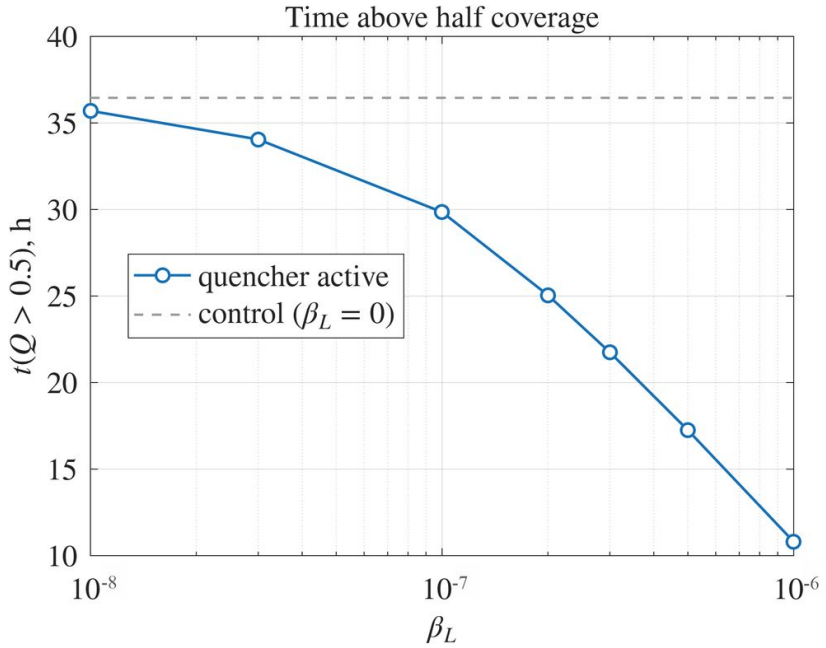


Figure 6: Duration $t_{0.5}$ of the on-state, i.e., the state in which more than half of the colony area exhibits active quorum sensing: Series A, dependence on the enzyme production rate of species 2 β_L, mol/(L·h), at $\varphi = 0.5$ (logarithmic scale on the horizontal axis); circles and solid line show the active quencher, dashed line shows the control $\beta_L = 0$.

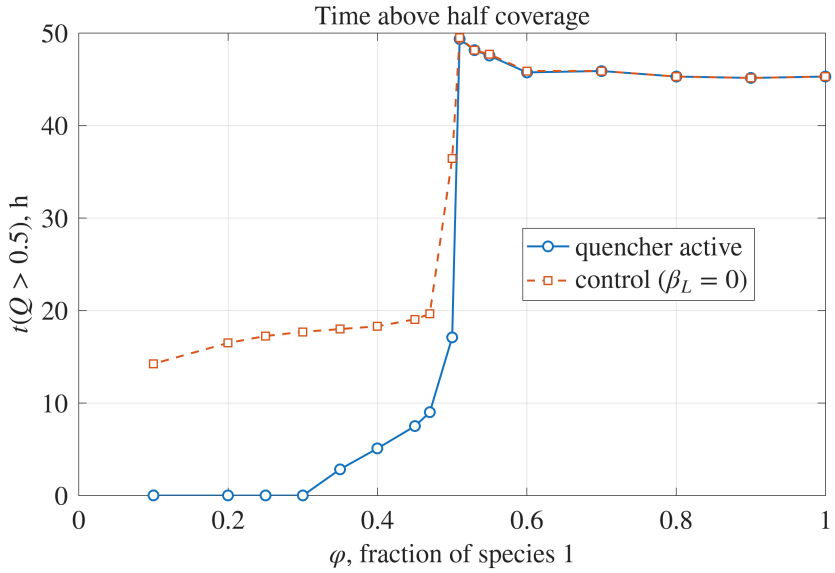


Figure 7: Duration $t_{0.5}$ of the on-state, i.e., the state in which more than half of the colony area exhibits active quorum sensing: Series B, dependence on the fraction φ of species 1 in the inoculum (dimensionless); circles and solid line show $\beta_L = 5.05 \cdot 10^{-7}$ mol/(L·h), squares and dashed line show the control $\beta_L = 0$.

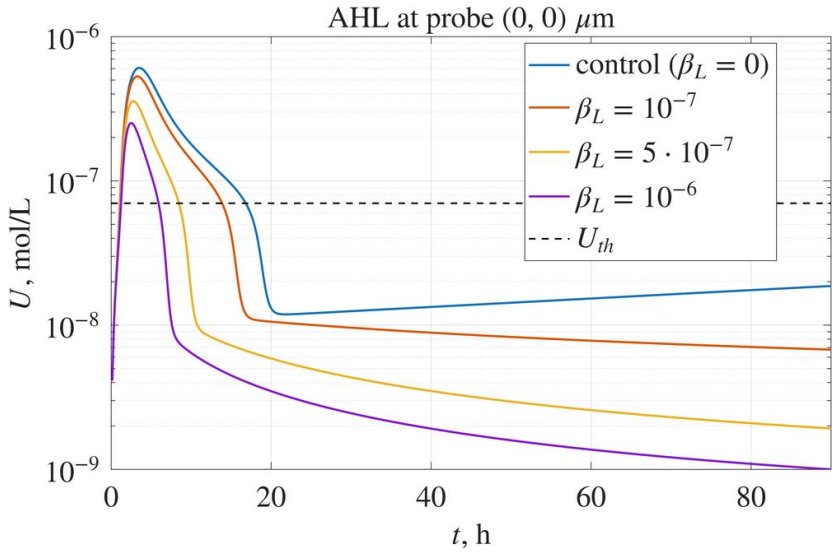


Figure 8: Time course of the AHL concentration U, mol/L, at the inoculation center for different enzyme production rates β_L of species 2, at $\varphi = 0.5$. The dashed line is the quorum threshold U_{th}. Logarithmic scale on the vertical axis, the time t is in hours.

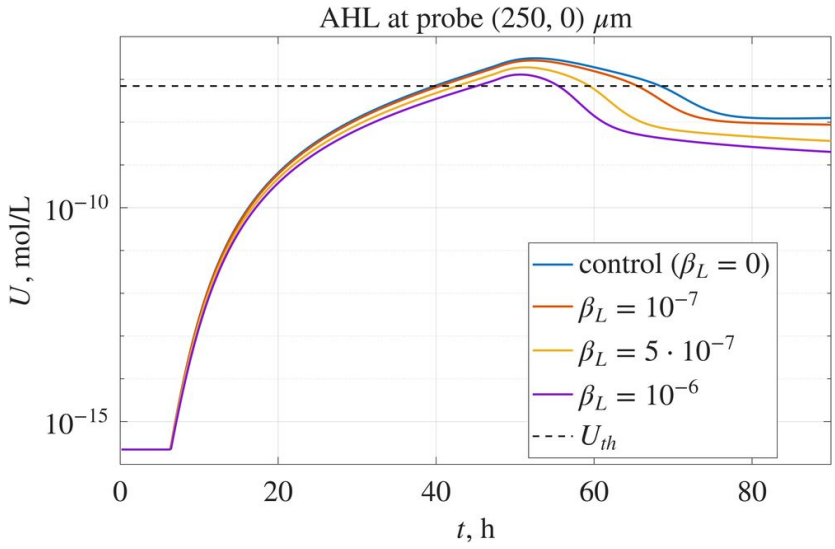


Figure 9: Time course of the AHL concentration U, mol/L, at a point 250 μm away from the inoculation center, which the colony front passes at about 50 h, for different enzyme production rates β_L of species 2, at $\varphi = 0.5$. The dashed line is the quorum threshold U_{th}. Logarithmic scale on the vertical axis, the time t is in hours.

6 Conclusion

We proposed a reaction-diffusion model of joint growth of two bacterial species on a nutrient medium which takes into account quorum sensing and quorum quenching. One species produces the signal and, with a delay, its own enzyme that degrades it; the other one does not take part in communication, but constantly secretes lactonase.

The computational experiments allow us to draw the following conclusions. Without quorum sensing, the outcome of competition is decided at the growth front: the species with lower motility or lower substrate consumption rate ends up in the depleted zone and stops growing. Quenching acts smoothly, not as a threshold, and reduces quorum rather than eliminating it: as enzyme production grows, the duration of the coordinated state decreases, but quorum still occurs. In space, quorum is kept at the growing front of the colony, while the enzyme accumulates in its center. The control simulation with the enzyme switched off makes it possible to separate quenching from competition. Two critical fractions of the signal producer in the inoculum separate three regimes: no effect at $\varphi \geq 0.51$, partial suppression at $0.35 \leq \varphi \leq 0.5$, and complete suppression at $\varphi \leq 0.3$.

The model has some limitations. The signal and the enzyme do not affect the growth and motility of the bacteria, so quorum sensing here is a passive indicator of the population state. Also, the quencher produces the enzyme at no cost, while in reality enzyme production requires resources. This cost can be taken into account, for example, by reducing the growth rate ν_{B2} in proportion to β_L. With such a cost, the quencher would probably lose the competition for the substrate more strongly, so the quorum suppression obtained here should be seen as an upper estimate. We plan to include these effects in future work.

The proposed approach can serve as a tool for preliminary evaluation of biological control strategies in which suppression of quorum-dependent virulence is achieved by introducing a quencher species rather than by direct action on the pathogen.

References

[1] M. Ananda, I. Rusmana, and A. Akhdiya. Quorum quenching of *Bacillus cereus* INT1c against Pseudomonas syringae. *Journal of Physics: Conference Series*, 1277:012010, 2019.

[2] A. K. Bhardwaj, K. Vinothkumar, and N. Rajpara. Bacterial quorum sensing inhibitors: attractive alternatives for control of infectious pathogens showing multiple drug resistance. *Recent Patents on Anti-Infective Drug Discovery*, 8(1):68–83, 2013.

[3] K. Buddrus-Schiemann, M. Rieger, M. Mühlbauer, M. V. Barbarossa, C. Kuttler, B. A. Hense, M. Rothballer, J. Uhl, J. R. Fonseca, P. Schmitt-Kopplin, M. Schmid, and A. Hartmann. Analysis of N-acylhomoserine lactone dynamics in continuous cultures of *Pseudomonas putida* IsoF by use of ELISA and UHPLC/qTOF-MS-derived measurements and mathematical models. *Analytical and Bioanalytical Chemistry*, 406:6373–6383, 2014.

[4] T. Defoirdt. Resistance to quorum sensing inhibition spreads more slowly during host infection than antibiotic resistance. *Gut Microbes*, 17(1):2476582, 2025.

[5] J. D. Dockery and J. P. Keener. A mathematical model for quorum sensing in Pseudomonas aeruginosa. *Bulletin of Mathematical Biology*, 63(1):95–116, 2001.

[6] Y.-H. Dong, A. R. Gusti, Q. Zhang, J.-L. Xu, and L.-H. Zhang. Identification of quorum-quenching N-acyl homoserine lactonases from *Bacillus species*. *Applied and Environmental Microbiology*, 68(4):1754–1759, 2002.

[7] Y.-H. Dong, L.-H. Wang, J.-L. Xu, H.-B. Zhang, X.-F. Zhang, and L.-H. Zhang. Quenching quorum-sensing-dependent bacterial infection by an N-acyl homoserine lactonase. *Nature*, 411(6839):813–817, 2001.

[8] Y.-H. Dong, J.-L. Xu, X.-Z. Li, and L.-H. Zhang. AiiA, an enzyme that inactivates the acyl-homoserine lactone quorum-sensing signal and attenuates the virulence of *Erwinia carotovora*. *Proceedings of the National Academy of Sciences USA*, 97(7):3526–3531, 2000.

[9] Y.-H. Dong, X.-F. Zhang, J.-L. Xu, and L.-H. Zhang. Insecticidal Bacillus thuringiensis silences Erwinia carotovora virulence by a new form of microbial antagonism, signal interference. *Applied and Environmental Microbiology*, 70(2):954–960, 2004.

[10] M. J. Federle and B. L. Bassler. Interspecies communication in bacteria. *Journal of Clinical Investigation*, 112(9):1291–1299, 2003.

[11] A. Fekete, C. Kuttler, M. Rothballer, B. A. Hense, D. Fischer, K. Buddrus-Schiemann, M. Lucio, J. Müller, P. Schmitt-Kopplin, and A. Hartmann. Dynamic regulation of N-acyl-homoserine lactone production and degradation in *Pseudomonas putida* IsoF. *FEMS Microbiology Ecology*, 72(1):22–34, 2010.

[12] A. B. Goryachev. Understanding bacterial cell-cell communication with computational modeling. *Chemical Reviews*, 111(1):238–250, 2011.

[13] T. Horger, C. Kuttler, B. Wohlmuth, and A. Zhigun. Analysis of a bacterial model with nutrient-dependent degenerate diffusion. *Mathematical Methods in the Applied Sciences*, 38(17):3851–3865, 2015.

[14] R. E. Kannan and S. Saini. Mathematical modelling of quorum sensing in bacteria. *INAE Letters*, 3:175–187, 2018.

[15] K. Kawasaki, A. Mochizuki, M. Matsushita, T. Umeda, and N. Shigesada. Modeling spatio-temporal patterns generated by *Bacillus subtilis*. *Journal of Theoretical Biology*, 188:177–185, 1997.

[16] C. Kuttler and A. Maslovskaya. Hybrid stochastic fractional-based approach to modeling bacterial quorum sensing. *Applied Mathematical Modelling*, 93:360–375, 2021.

[17] T. Maeda, R. García-Contreras, M. Pu, L. Sheng, L. R. Garcia, M. Tomás, and T. K. Wood. Quorum quenching quandary: resistance to antivirulence compounds. *The ISME Journal*, 6(3):493–501, 2012.

[18] A. Maslovskaya, C. Kuttler, A. Chebotarev, and A. Kovtanyuk. Optimal multiplicative control of bacterial quorum sensing under external enzyme impact. *Mathematical Modelling of Natural Phenomena*, 29:1–15, 2022.

[19] A. Maslovskaya, C. Kuttler, I. Shevkun, A. Chebotarev, and A. Kovtanyuk. Quorum sensing model for nutrient-dependent evolution of cultured bacteria: theoretical framework and in silico study. *Nonlinear Dynamics*, 113:7519–7534, 2025.

[20] A. Maslovskaya, I. Shevkun, and C. Kuttler. The evolution model of cultured bacteria with external growth inhibition: computational techniques and in silico studies. In *Proceedings of 3rd International Workshop on Mathematical Modeling and Scientific Computing*, volume 104 of *EPiC Series in Computing*, pages 209–220, 2024.

[21] M. B. Miller and B. L. Bassler. Quorum sensing in bacteria. *Annual Review of Microbiology*, 55:165–199, 2001.

[22] J. Müller, C. Kuttler, B. A. Hense, M. Rothballer, and A. Hartmann. Cell-cell communication by quorum sensing and dimension-reduction. *Journal of Mathematical Biology*, 53(4):672–702, 2006.

[23] J. Perez-Velazquez, M. Gölgeli, and R. Garcia-Contreras. Mathematical modelling of bacterial quorum sensing: a review. *Bulletin of Mathematical Biology*, 78:1585–1639, 2016.

[24] N. C. Reading and V. Sperandio. Quorum sensing: the many languages of bacteria. *FEMS Microbiology Letters*, 254(1):1–11, 2006.

[25] K. Saurav, R. Bar-Shalom, M. Haber, I. Burgsdorf, G. Oliviero, V. Costantino, D. Morgenstern, and L. Steindler. In search of alternative antibiotic drugs: quorum-quenching activity in sponges and their bacterial isolates. *Frontiers in Microbiology*, 7:416, 2016.

[26] J. A. Shapiro. Control of *Pseudomonas putida* growth on agar surfaces. In J. R. Sokatch, editor,

The Bacteria, volume X, pages 27–69. Academic Press, New York, 1986.

[27] I. Shevkun and A. Maslovskaya. Efficient parallel computational techniques for implementing a reaction-diffusion model of bacterial growth in media. In L. Sokolinsky et al., editors, *Parallel Computational Technologies. PCT 2025*, volume 2891 of *Communications in Computer and Information Science*, pages 440–453, Cham, 2026. Springer.

[28] C. H. Tan, H.-S. Oh, V. M. Sheraton, E. Mancini, S. C. J. Loo, S. Kjelleberg, P. M. A. Sloot, and S. A. Rice. Convection and the extracellular matrix dictate inter- and intra-biofilm quorum sensing communication in environmental systems. *Environmental Science & Technology*, 54(11):6730–6740, 2020.

[29] J. P. Ward, J. R. King, A. J. Koerber, P. Williams, J. M. Croft, and R. E. Sockett. Mathematical modelling of quorum sensing in bacteria. *IMA Journal of Mathematics Applied in Medicine and Biology*, 18(3):263–292, 2001.

[30] N. N. Yanenko. *The Method of Fractional Steps: Solution of Problems of Mathematical Physics in Several Variables*. Springer, New York, 1971.